

Differential cross sections for electron-impact excitation of hydrogenlike ions

Shinobu Nakazaki* and Yukikazu Itikawa

Institute of Space and Astronautical Science, Yoshinodai, Sagami-hara 229, Japan

(Received 21 December 1988)

A systematic study is made of differential cross sections for the electron-impact excitation of the $2s$ and $2p$ states of H-like ions. The cross section is calculated in the Coulomb-Born and the Coulomb-Born-Oppenheimer approximations. A comparison of the resulting cross sections is made along the isoelectronic sequence from $Z = 1$ to ∞ (Z being the nuclear charge) to reveal the role of the Coulomb force in the excitation processes. For the $1s$ - $2p$ transition, the behavior of the apparent generalized oscillator strength for the ions is found to be different from that for neutral hydrogen.

I. INTRODUCTION

Differential cross sections (DCS) are fundamental quantities in understanding the reaction mechanism of electron-impact excitation of atoms and molecules. In the case of electron-ion collisions, there have been no thorough investigations of the DCS. It is difficult to obtain experimental DCS for electron-ion collisions. Theoretical results of DCS have been occasionally reported, sometimes as a byproduct of the calculation of the integrated cross section. The present paper reports a systematic study of DCS for the electron-impact excitation of H-like ions.

The study of electron collisions with H-like ions is of fundamental importance since these systems are the simplest examples of electron-ion collisions. For instance, there is no ambiguity about the accuracy of the target wave function, which is of importance in the study of electron-ion collisions. The DCS for the excitation of some H-like ions have previously been calculated.¹⁻¹¹ However, most of the calculations were made only for He^+ . Here we present a systematic study of the DCS along the entire isoelectronic sequence (including neutral H). The DCS for the $1s$ - $2s$, $2p$ excitations are calculated for several ions of the H-like sequence using the

Coulomb-Born (CB) and the Coulomb-Born-Oppenheimer (CBO) approximations. These methods may not give accurate results at the energies near threshold, especially for lower charged ions. They can be used, however, to show the characteristic trends of the cross section along the isoelectronic sequence.

There have been no reported measurements of the DCS for any H-like ion. Considering the fundamental nature of such collisions, it would be desirable to perform an experiment to measure the DCS for H-like ions. The present calculation could serve as a guide for the planning of such an experiment.

II. THEORY

Detailed formulas for the DCS for the excitation of ions are shown in a recent paper.¹² The DCS at scattering angle θ for the excitation process $\alpha \rightarrow \beta$ is given by (atomic units being used throughout the present paper)

$$\frac{d\sigma(\alpha \rightarrow \beta)}{d\omega} = \sum_{\nu=0}^{\infty} A_{\nu}(\alpha \rightarrow \beta) P_{\nu}(\cos\theta), \quad (2.1)$$

where P_{ν} is the Legendre function and

$$A_{\nu}(\alpha \rightarrow \beta) = \frac{1}{8k_{\alpha}^2} \frac{1}{(2L^{\alpha} + 1)(2S^{\alpha} + 1)} \sum_S (2S + 1) \sum_l \sum_{l'} \sum_{\bar{l}} \sum_{\bar{l}'} \sum_j B(l l' \bar{l} \bar{l}' j \nu) T_{l'}^j(\alpha \rightarrow \beta) T_{\bar{l}'}^j(\alpha \rightarrow \beta)^* . \quad (2.2)$$

Here $L^{\alpha} S^{\alpha}$ ($L^{\beta} S^{\beta}$) are the orbital and spin angular momenta of the initial (final) state of the target ion, l (l') is the orbital angular momentum of the incident (scattered) electron, j is the angular momentum transferred during the collision, and LS are the total orbital and spin angular momenta of the e^- ion system. The wave number of the incident (scattered) electron is denoted by k_{α} (k_{β}).

The coefficient B is defined in terms of the 3- j and 6- j symbols as

$$B(l l' \bar{l} \bar{l}' j \nu) = i^{l-l'+\bar{l}-\bar{l}'} (-1)^{j+\nu} (2j+1)(2\nu+1) \begin{Bmatrix} l & \bar{l} & \nu \\ 0 & 0 & 0 \end{Bmatrix} \begin{Bmatrix} l' & \bar{l}' & \nu \\ 0 & 0 & 0 \end{Bmatrix} \begin{Bmatrix} l & \bar{l} & \nu \\ \bar{l}' & l' & j \end{Bmatrix} . \quad (2.3)$$

The matrix element $T_{l'l'}^j$ in Eq. (2.2) is given by

$$T_{l'l'}^j(\alpha \rightarrow \beta) = \sum_L (-1)^L (2L+1) [(2l+1)(2l'+1)]^{1/2} (-1)^{-l-l'-L\alpha-L\beta} \begin{Bmatrix} l & L^\alpha & L \\ L^\beta & l' & j \end{Bmatrix} \exp[i(\rho_l^{(\alpha)} + \rho_{l'}^{(\beta)})] T_{l'l'}^{LS}(\alpha \rightarrow \beta), \quad (2.4)$$

where $\rho_l^{(s)}$ is the Coulomb phase shift [$\rho_l^{(s)} = \arg\Gamma(l+1-iq/k_s)$, q being the ionic charge]. In the present Coulomb-Born (CB) and Coulomb-Born-Oppenheimer (CBO) calculations, the transition matrix element $T_{l'l'}^{LS}$ in Eq. (2.4) is calculated with the following formulas:

$$T_{l'l'}^{LS} = -2iR_{ll'}^{LS} = -2i[R^d + (-1)^S R^e] \quad (2.5)$$

with

$$R^d = -2 \sum_\lambda \langle l'l^\beta L | P_\lambda | lL^\alpha \rangle D_\lambda, \quad (2.6)$$

and

$$R^e = -2(-1)^{l+L\alpha-L} \sum_\lambda \langle L^\beta l'l | P_\lambda | lL^\alpha \rangle E_\lambda. \quad (2.7)$$

Here D_λ (E_λ) is the direct (exchange) part of the radial integral over the target orbitals and the Coulomb continuum. Detailed expressions for D_λ , E_λ , and the matrix element of P_λ are given by Burgess *et al.*¹³

In the actual calculation of the DCS, we employ the computer code developed by Salvini.¹⁴ The original version of this code was found to contain some errors when applied to an electron-ion collision. (Actually the original code of Salvini does not correctly take into account the Coulomb phase.) A corrected code was used for the present calculations. The convergence of the partial wave expansion is slower for the DCS than for the integrated cross section, particularly for the dipole-allowed transitions. Therefore, the contributions of the higher partial waves for the DCS calculation should be taken into account very carefully. The radial integrals (D_λ) for the monopole and dipole contributions were evaluated using the analytical method of Nakazaki.¹⁵ With that procedure, we can avoid numerical integration involving the Coulomb function and the long-range tail of dipole interaction, which becomes more tedious for higher partial waves. The maximum total angular momentum L considered in the present calculation was 60 for the dipole transition. The present DCS for the $1s$ - $2s$ and $1s$ - $2p$ transitions in He^+ at twice the threshold energy agree with those of Mitra and Sil⁴ and Deb *et al.*,¹¹ who evaluated the CB matrix element without recourse to a partial wave expansion, but using numerical integration in the evaluation of each matrix element.

III. RESULTS

A. $1s$ - $2s$

Figure 1 shows the DCS for the $1s$ - $2s$ transition calculated by the Coulomb-Born method for several members of the H-like isoelectronic sequence. To compare the

cross section for different ions, a scaled DCS, $Z^4 d\sigma/d\omega$ (Z being the nuclear charge) is plotted against the scattering angle θ for the same electron energy X in threshold units. The DCS in Fig. 1 are calculated at $X=2$ (i.e., twice the threshold energy). The DCS is also shown for the limit $Z \rightarrow \infty$. The procedure used to obtain the limiting value is the same as described by Burgess *et al.*¹³ We also present in Fig. 1 the cross section for the other limit of the isoelectronic sequence; namely neutral hydrogen (H). The plane-wave Born (PB) approximation is used to get the cross section for H.

Figure 1 shows the systematics of the DCS along the isoelectronic sequence. The Coulomb force exerted by the target ion affects the scattering more at large angles than at small angles. The scaled DCS for the ions converge rapidly and uniformly as $Z \rightarrow \infty$. The scaled DCS for $Z=6$, for example, is no more than 30% different from the value at $Z \rightarrow \infty$. For all the ions along the H-like sequence (including H itself), the PB method gives the same DCS, provided it is scaled as $Z^4 d\sigma/d\omega$ and calculated at the same energy X . The difference between the PB curve and the other ones gives an indication of the er-

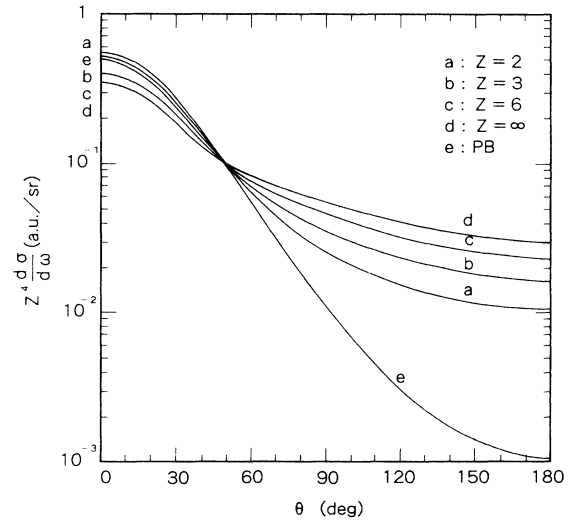


FIG. 1. Differential cross sections (in a.u./sr or equivalently in units of a_0^2/sr , a_0 being the Bohr radius) for the $1s$ - $2s$ excitation of H-like ions of (a) $Z=2$ (Z being the nuclear charge), (b) $Z=3$, (c) $Z=6$, and (d) $Z=\infty$, calculated using the Coulomb-Born (CB) method. For comparison, the corresponding cross section for H, calculated with the plane-wave Born (PB) method, is also shown (e). All the calculations were carried out at the electron energy $X=2$. The cross section multiplied by Z^4 is plotted against the scattering angle.

rors introduced by using the PB approximation instead of the CB approximation in the calculation of the DCS for ions.

Figure 2 shows the same DCS as in Fig. 1, but for a higher energy ($X=3$). As the collision energy increases, the forward scattering is enhanced. Other features of the DCS plotted in Fig. 2 are similar to those seen in Fig. 1.

The effects of electron exchange in the $1s$ - $2s$ excitation are seen in Figs. 3 and 4, where the cross sections calculated with (i.e., CBO) and without (i.e., CB) electron exchange for $Z=2$ and $Z=\infty$ are compared at $X=2$. For $Z=2$, exchange has a large effect for $\theta > 100^\circ$. In the limit $Z \rightarrow \infty$, the exchange effect is smaller but still cannot be ignored. It is interesting to see that the relative size of the effect in $Z \rightarrow \infty$ is almost the same at all scattering angles.

B. $1s$ - $2p$

Figures 5 and 6 show the DCS for $1s$ - $2p$ transition calculated by the CB method at $X=2$ and 3, respectively. Figures 7 and 8 compare the CB and CBO results for the $1s$ - $2p$ transition for $Z=2$ and ∞ at $X=2$. Except for the strong forward scattering, the DCS for the $1s$ - $2p$ excitation have characteristics similar to those for the $1s$ - $2s$ excitation.

One peculiar feature of the DCS for the $1s$ - $2p$ transition shown in Fig. 5 is that, with increasing nuclear charge, the peak at $\theta=0^\circ$ flattens and the peak position moves to a larger angle. This trend is less clear, but still discernible, at the higher collision energy ($X=3$) shown in Fig. 6. Small-angle scattering for the $1s$ - $2p$ transition is dominated by the long-range (dipole) interaction. Electrons passing the target at large-impact parameters are deflected by the Coulomb force. As the Coulomb force increases, forward scattering becomes suppressed. This is a very naive explanation of the peak shift in the DCS shown in Figs. 5 and 6.

In the study of the DCS for neutral atoms or molecules, comparison with the generalized oscillator strength

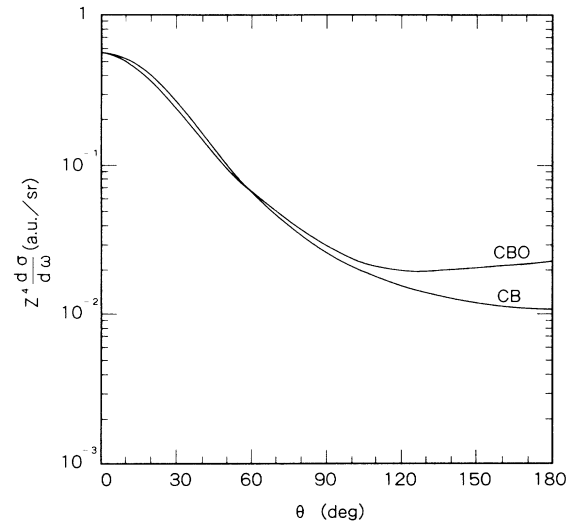


FIG. 3. Comparison of the differential cross sections for the $1s$ - $2s$ excitation of He^+ ($Z=2$) calculated with the CB and the CBO methods at $X=2$.

(GOS) often serves as a useful benchmark. Here we introduce an “apparent” GOS defined by¹⁶

$$F(K, E) = \frac{k_\alpha}{4k_\beta} K^2 [\Delta E (\text{Ry})] \frac{d\sigma}{d\omega} \text{ (a.u./sr)}, \quad (3.1)$$

where K is the momentum transfer. When the DCS calculated in the PB approximation is inserted into the right-hand side of Eq. (3.1), the quantity $F(K, E)$ reduces to the GOS and becomes independent of the incident energy E . From the DCS given in Figs. 5 and 6, we evaluate $F(K, E)$ for the $1s$ - $2p$ transition in various ions. Some typical values of the scaled quantity $F/(\Delta E/Z^2)$ as a function of $(K/Z)^2$ are shown in Fig. 9. The solid line

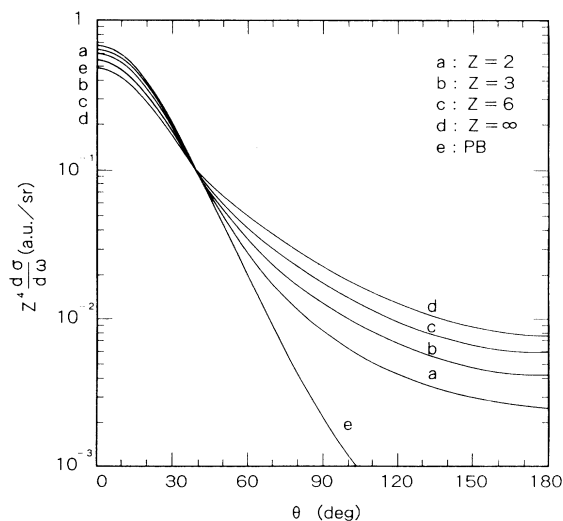


FIG. 2. The same as Fig. 1 (i.e., $1s$ - $2s$ excitation), but for $X=3$.

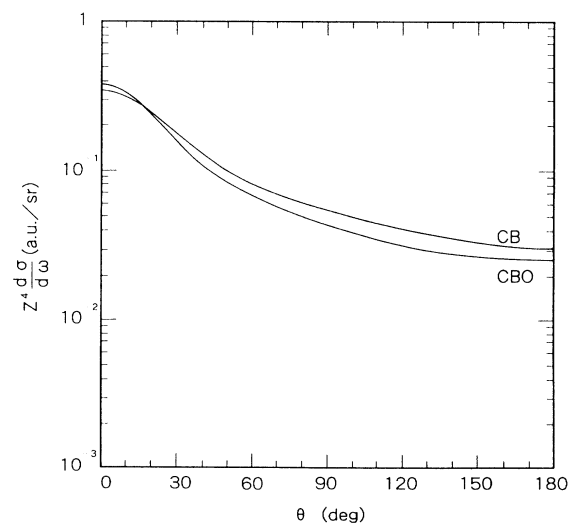


FIG. 4. The same as Fig. 3 (i.e., $1s$ - $2s$ excitation at $X=2$), but for the ion with $Z=\infty$.

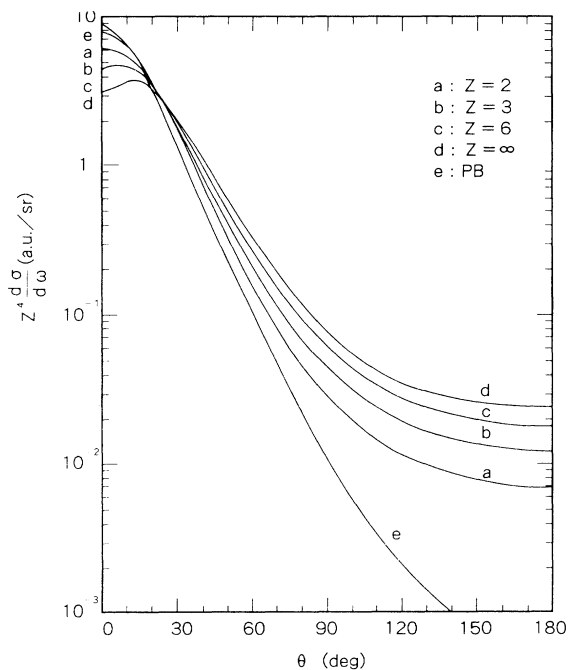


FIG. 5. The same as Fig. 1 (i.e., the CB calculation at $X=2$), but for the $1s-2p$ transition.

in Fig. 9 is the GOS for H. It also represents the GOS for any ion of the H-like isoelectronic sequence. The figure shows that in the small-angle region, the “apparent” GOS decreases with decreasing K . This corresponds to the flattening of the forward peak in the DCS shown in Figs. 5 and 6. (The leftmost point of each data

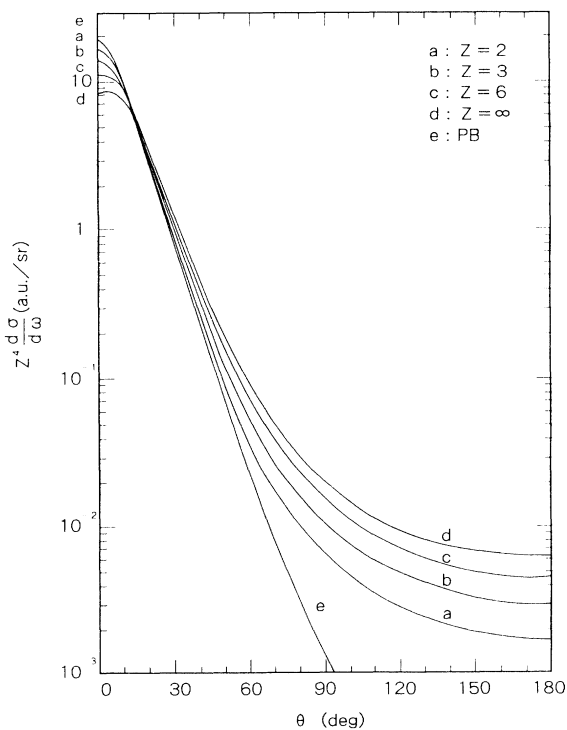


FIG. 6. The same as Fig. 5 (i.e., the CB calculation for $1s-2p$ excitation), but for $X=3$.

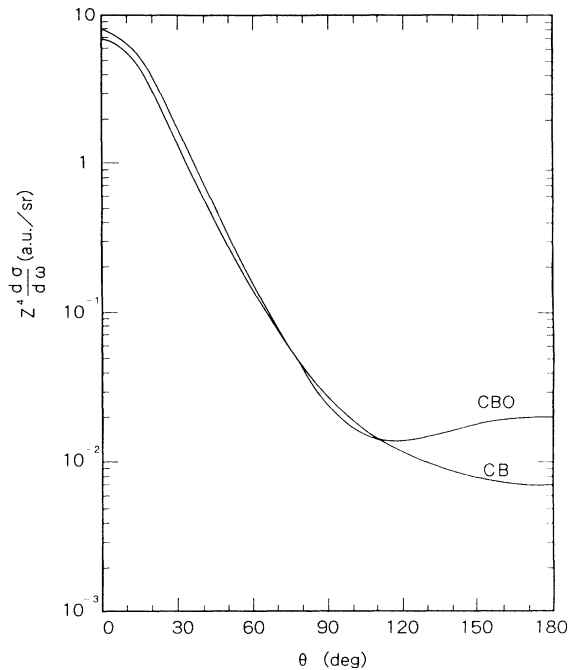


FIG. 7. The same as Fig. 3 (i.e., $Z=2$ and $X=2$), but for the $1s-2p$ transition.

set corresponds to $\theta=0^\circ$.) The deviation of F from the GOS curve in the small- K region becomes larger as Z increases and smaller as the collision energy increases. From this figure, it appears that the Lassettre's theorem (F approaches the optical oscillator strength as K or $K^2 \rightarrow 0$ irrespective of E)¹⁷ does not hold in this case.

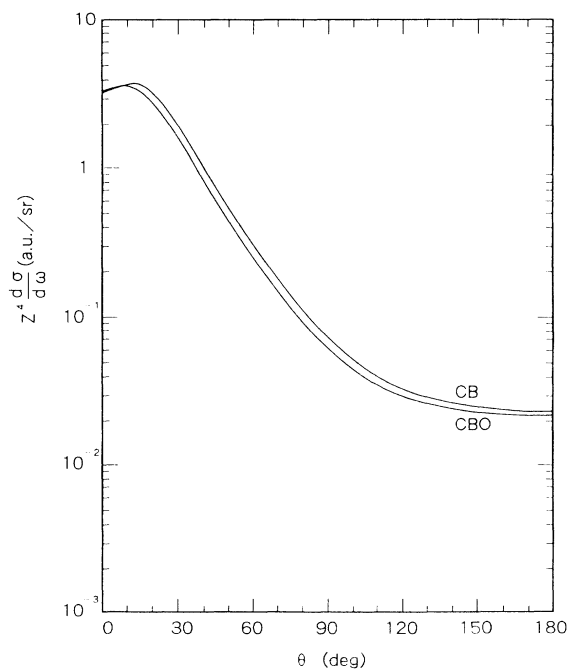


FIG. 8. The same as Fig. 4 (i.e., $Z=\infty$ and $X=2$), but for the $1s-2p$ transition.

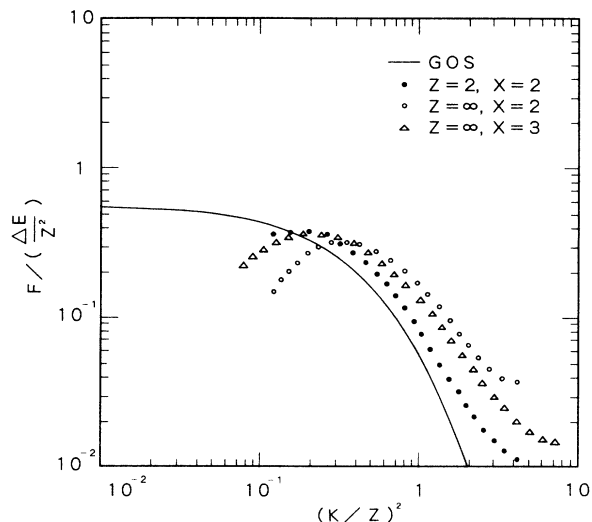


FIG. 9. Apparent generalized oscillator strengths (scaled by $\Delta E/Z^2$) for the $1s-2p$ transition in H-like ions derived from the differential cross sections shown in Figs. 5 and 6. The abscissa indicates the momentum-transfer squared (scaled by Z^2). The solid line shows the corresponding generalized oscillator strength for H (and any H-like ion).

This phenomenon has already been noted by Mitroy^{18,19} for electron-impact excitation of the resonant transitions in Mg^+ and Be^+ . In this respect, it would be of interest to study the DCS for other isoelectronic sequences.

IV. CONCLUDING REMARKS

The differential cross sections (DCS) for the $1s-2s, 2p$ transitions for H-like ions have been studied systematically as a function of nuclear charge (Z). It has been shown how the DCS is affected by the Coulomb force, which is an essential part of the electron-ion interaction. The calculation was made with the Coulomb-Born and the Coulomb-Born-Oppenheimer approximations. Although the CB and the CBO methods are expected to give results approaching those of the close-coupling method as Z or X (electron energy in threshold units) increases, they are sometimes inaccurate in the vicinity of the excitation threshold, especially for ions with small nuclear charge. When compared to the (integrated) cross section recommended by Callaway²⁰ (mostly based on the close-coupling calculation), the CBO method gives a good cross section for the $1s-2p$ excitation in He^+ ($Z=2$) at any energy. For the $1s-2s$ excitation, the CBO is very poor for $Z=2$ at $X=2$, but gets better as Z or X increases. The present result shown in the previous section can be used to deduce the systematic trend of the DCS, except for the $1s-2s$ transition of the ions with small Z . It would be very interesting to make a similar study of DCS with a more elaborate calculation, and perhaps to study ions of another isoelectronic sequence.

ACKNOWLEDGMENTS

The authors would like to thank K. Sakimoto for his helpful discussions.

*Permanent address: Department of Applied Physics, Faculty of Engineering, Miyazaki University, Miyazaki 889-21, Japan.

¹M. R. C. McDowell, L. A. Morgan, and V. P. Myerscough, *J. Phys. B* **6**, 1435 (1973).

²A. D. Stauffer and L. A. Morgan, *J. Phys. B* **8**, 2172 (1975).

³C. A. Weatherford, *J. Phys. B* **9**, L135 (1976).

⁴C. Mitra and N. C. Sil, *Phys. Rev. A* **14**, 1009 (1976).

⁵P. R. Simony, J. H. McGuire, J. E. Golden, and B. R. Junker, *Phys. Rev. A* **16**, 1401 (1977).

⁶C. Mitra and N. C. Sil, *Phys. Rev. A* **18**, 1758 (1978).

⁷C. Sinha, N. Roy, and N. C. Sil, *J. Phys. B* **11**, 1807 (1978).

⁸C. Sinha and N. C. Sil, *J. Phys. B* **12**, 1711 (1979).

⁹S. N. Singh, S. Kumar, and M. K. Srivastava, *J. Phys. B* **12**, 2351 (1979).

¹⁰K. A. Berrington, A. E. Kingston, and S. A. Salvini, *J. Phys.*

B **16**, 2399 (1983).

¹¹N. C. Deb, C. Sinha, and N. C. Sil, *Phys. Rev. A* **27**, 2447 (1983).

¹²Y. Itikawa and K. Sakimoto, *Phys. Rev. A* **38**, 664 (1988).

¹³A. Burgess, D. G. Hummer, and J. A. Tully, *Philos. Trans. R. Soc. London, Ser. A*: **266**, 225 (1970).

¹⁴S. A. Salvini, *Comput. Phys. Commun.* **27**, 25 (1982). The original version of Salvini's code contains some errors.

¹⁵S. Nakazaki, *J. Phys. Soc. Jpn.* **45**, 225 (1978).

¹⁶M. Inokuti, *Rev. Mod. Phys.* **43**, 297 (1971).

¹⁷E. N. Lassettre, A. Skerbele, and M. A. Dillon, *J. Chem. Phys.* **50**, 1829 (1969).

¹⁸J. Mitroy, *Phys. Rev. A* **37**, 649 (1988).

¹⁹J. Mitroy, *J. Phys. B* **21**, L25 (1988).

²⁰J. Callaway, *Phys. Lett.* **96A**, 83 (1983).